Relative Importance of Rock Mass Geometrical Parameters on Erosion in a Dam Spillway Tailrace using a Small-Scale Physical Model 2022

Marie-Hélène Wisse and Ali Saeidi
Department of Applied Sciences – Université du Québec à Chicoutimi, Chicoutimi, Quebec, Canada
Marco Quirion
Hydro-Québec, Montreal, Quebec, Canada

GeoCalgary 2022 October 2-5
Reflection on Resources

RÉSUMÉ
Les évacuateurs de crues des barrages sont à risque d'érosion dû à l'excavation du massif rocheux ainsi qu'aux forts débits appliqués à la roche non recouverte. Des études portant sur ce sujet ont déjà été réalisées, mais certains aspects comme la relation entre les paramètres d'érosion du massif rocheux demeurent incertains. Pour étudier cela, un modèle à échelle réduit d'un évacuateur de crues, qui reproduit le débit d'écoulement et les dimensions du modèle réel, a été construit dans un laboratoire de l'Université du Québec à Chicoutimi. Ce modèle permet de simuler le massif rocheux au sein d'un canal d'écoulement avec des blocs de béton de taille, disposition et densité variables. Les objectifs des essais sont de déterminer l'effet relatif des paramètres géométriques du massif rocheux sur son érodabilité : l'ouverture des joints, la saillie des blocs, l'orientation des joints, l'espacement des joints et le volume des blocs.

ABSTRACT
Dams spillway tailrace are at risk of erosion, given the excavation of the rock mass, as well as due to the high flow rates applied to the unlined rock. Studies have already been carried out on the subject, but several aspects, including the relationship between the erosion parameters, remain uncertain. To study this problem, a small-scale model of a spillway, which reproduced the flow rate and the real model dimensions, was built in a laboratory of the University of Quebec at Chicoutimi (UQAC). This model allows the simulation of the rock mass in the flow channel with concrete blocks of variable size, layout and density. Different parameters of the rock mass are simulated using these blocks. The objective of these tests is to assess the relative effect of the geometric parameters of the rock mass on erosion, such as joint opening, block protrusion, joint orientation, joint spacing and block volume.

1 INTRODUCTION

Spillways are used to evacuate excess water in dam reservoirs. They consist of channels excavated in the bed rock. The excavation process as well as the natural discontinuities of the rock mass, coupled with hydraulic characteristics of the flow in the channel as high flow velocity and turbulence can make the rock mass vulnerable to erosion. Erosion of rock mass in high velocity flow channels is due to pressure variations on the top and bottom of blocks. When upward forces due to high flow velocity in the joints becomes higher than downward forces due to the weight of the block, the friction and the water pressure above the block, lifting of the block occur (Bollaert and Schleiss 2002; Pan et al. 2014). In empirical methods, erosion is defined as the limit where the flow power becomes greater than the resistance of rock mass to erosion. The resistance of rock mass to erosion is defined by different authors who use different rock mass parameters. Kirsten (1982) and Pells (2016) developed rock mass erodibility indices. Kirsten's Index (N) was used by different authors (Annandale 1995; Kirsten et al. 2000; Van Schalkwyk et al. 1994) to define an erodiblity threshold. The results obtained varied for each study. The Kirsten Index was first developed to assess rock mass excavatability rather than erodiblity, which could lead to some discrepancies in the evaluation of rock mass erodibility. For example, the excavation force was considered a bulldozer rather than flow power. The pressure applied by a bulldozer is on a very limited surface, counter to flow power, where water pressure is applied on all submerged surfaces of rock blocks. Pells (2016) developed the erodibility Geological Strength Index (eGSI) and the Rock Mass Erodibility Index (RMEI). The former adds an erodiblity parameter (E_{doa}) based on joint orientation to the Geological Strength Index GSI, while the latter is based solely on visual observation of rock mass erosion in unlined spillways. For these two indices, classification of erosion degrees errors for spillway erosion varies between 15% and 75% (Boumaiza et al. 2021).

The effects of rock mass characteristics on its erodibility are still less documented. More specifically, relative effect of joint orientation, joint opening, protrusion, block size and shape as well as joint shear strength are parameters known to have an effect on rock mass erosion in spillway channels (Boumaiza et al. 2019). Because of a lack of a comprehensive database on the erosion process combined to measurement difficulties of the effect of several parameters at in-situ scale, a physical small-scale model could be a very good tool for studying the effects of these parameters.

Previous physical flow model channels were built to study erodibility of rock mass in unlined spillway, as Reinius' model (1986), Annandale's model (1998), George

et al.'s model (2015) and Pells' model (2016). A literature review on the subject revealed that none of these physical models allow studying all relevant geomechanical characteristics of the rock mass having an effect on rock mass erodibility in the case of parallel-flow spillway channels.

For this study, a physical small-scale model of an existing spillway parallel-flow channel tailrace was built in a laboratory of the University of Quebec at Chicoutimi (UQAC). This model allows various configurations of rock mass to study its geometric characteristics as well as hydraulic characteristics of the flow. Beside studying hydraulic parameters, this model will be used to study the effects of geometric and geomechanical parameters of the rock mass, as joint opening, protrusion, joint orientation, joint spacing and block volume on their effect on rock mass erosion in unlined spillways tailrace.

In this paper, the physical small-scale model is presented as well as the methodology used to measure pressure on the instrumented block. The results are then presented and briefly explained. This paper ends with a conclusion summarizing the results and explaining future works that will be undergone with the physical small-scale model.

Some tests have already been driven and this article discusses results obtained by varying joint opening, protrusion of blocks and flow velocity.

2 MATERIALS AND METHODS

In order to accurately represent flow conditions of the real spillway, the pilot-plant-scaled model was built at a Froude number scale of 1:40 (Koulibaly 2021). The pump used allowed a flow rate up to 400 L/s. For the representativeness of the tests, flow velocity in the scaled-model channel was calculated according to the real spillway flow velocity of 20 m/s. With a Froude number scale of 1:40, the flow velocity required is 3.16 m/s. For the tests, various flow velocity from 3.2 m/s to 4.8 m/s were used. Two floodgates, designed as is in the real model, with adjustable openings allowed water to flow from the upstream basin to the channel. The channel had a length of 4.2 m, a width varying from 0.68 m to 0.87 m and a constant inclination of 9˚. Figures 1 and 2 show a sketch and a photograph of small-scaled physical model.

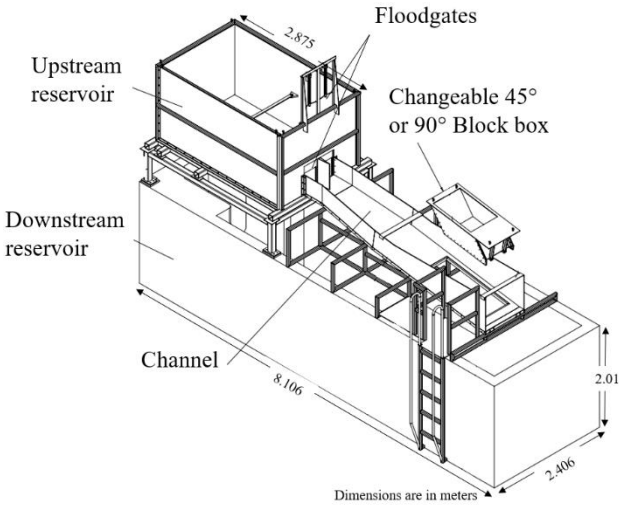

Figure 1: Sketch of the scaled physical model

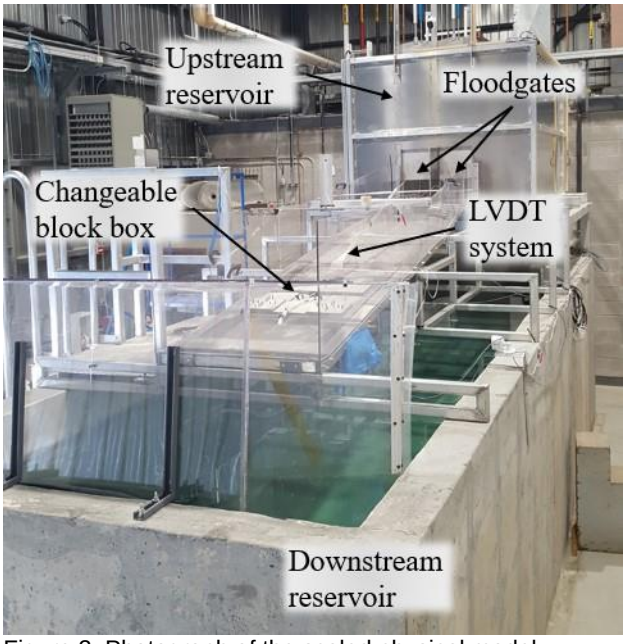

Figure 2: Photograph of the scaled physical model

Rock mass was represented by nine (9) concrete blocks placed in a mould at the end of the channel tailrace. One of these blocks was instrumented. For this purpose, the block was designed with built-in copper tubes. On each face, were placed two water entries flush to the surface of the block, for a total of twelve (12) water entries. All water exits were placed at the top of the block. Figure 3 shows the position of the water entries (blue arrows) and exits (orange arrows) as well as the interior design of the blocks.

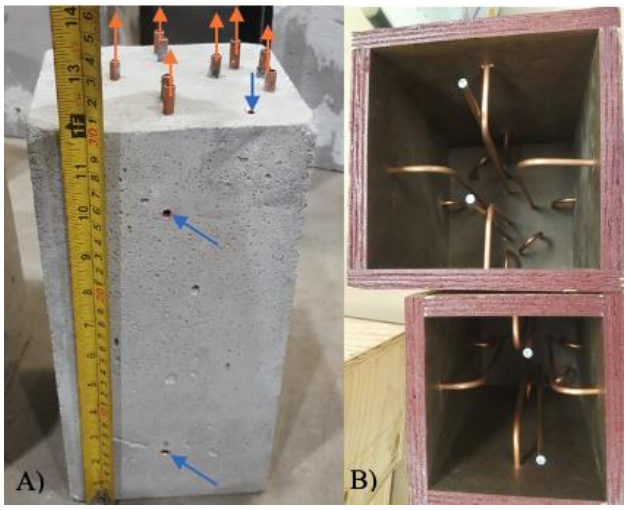

Figure 3: A) Position of the water entries in blue and exits in orange B) Design of the built-in copper tubes inside the blocks' moulds

The water exits were connected with stiff plastic tubes to pressure sensors placed outside the channel. When the joint opening of the blocks' configuration was large enough, a Pitot tube was used to measure flow velocity in the joints of the blocks. A Linear Variable Differential Transformer (LVDT) sensor was used to measure the variation of the water level on the channel, upstream of the blocks. To vary joint opening, two sizes of blocks were used (20x20x30 cm^3 and 15x15x30 cm^3). They allowed to have a joint opening respectively of 1 mm and about 40 mm. When larger joint opening is used, spacing bolts are used to maintain the opening during the tests. For further tests, joint opening for the 15x15x30 cm^3 blocks will be reduced to having a variety of values between 1 mm and 40 mm. Figure 4 shows a photograph the blocks placed in the 90-degree block box, for a 1 mm joint opening and a 38 mm joint opening. Water entries C, A and D are respectively placed on the upstream side of the instrumented block, on the top and on the downstream side.

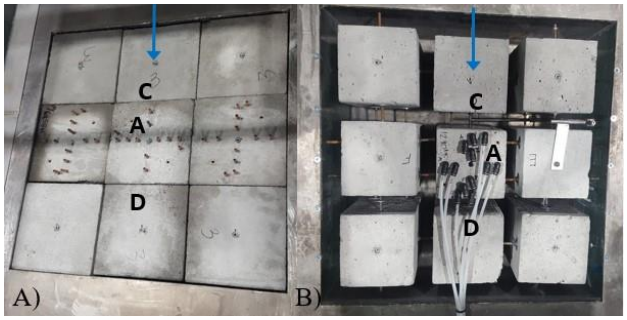

Figure 4: Photographs of the blocks' disposition A) With a joint opening of 1 mm using 20x20x30 cm^3 blocks B) With a joint opening of 38 mm using 15x15x30 cm^3 blocks

Protrusion was modified using spacing bolts under the blocks. Various configurations were used: ascendant stairs, descendant stairs, middle row protruding and upstream and downstream rows protruding. Values of joint openings have the precision of ± 2 mm and spacing used for protrusion are accurate at ± 1 mm. Figure 5 shows a protrusion example for the middle row of blocks. Water entry B is positioned under the block.

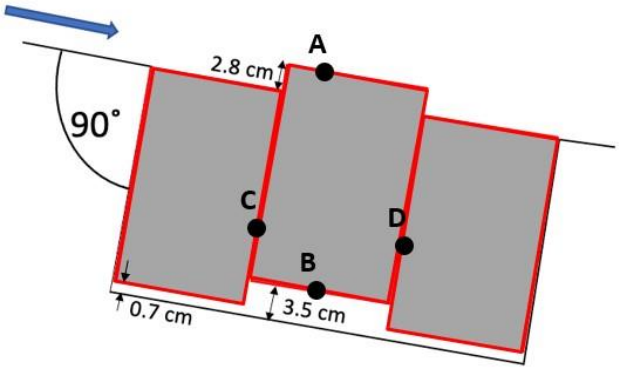

Figure 5: Sketch of the blocks in the 90-degree block box (side view) and position of the water entries A, C, D and B. The configuration shown has a 1 mm joint opening and 28 mm protrusion for the centre block (0-28-0).

The water entries on the block only measure the static pressure rather than the total pressure on the block's faces. The total pressure is known to be the sum of the static pressure, induced by the water head above the measuring position, and the dynamic pressure. The dynamic pressure is calculated with the square of the water velocity (v) divided by 2 times the gravitational acceleration (g): $v^2/2g$. In fluid mechanics, velocity of a fluid on a surface is assumed to be zero. Moreover, in order to accurately measure flow velocity, it is necessary that the water entries be parallel to the flow, in the opposite way so that water pressure caused by water velocity can enter the tube. However, in the blocks, the water entries are positioned perpendicular to the surface of each side of the block and are flush to the surface of each side. That is why we consider that the pressure sensors only measure static water pressure with each water entry.

3 PRELIMINARY RESULTS

Preliminary tests were run with blocks placed in the 90-degree block box, where the joint orientation of the top of the blocks is the same as the orientation of the channel surface. Joint opening was varied with two values, 1 mm and 38 mm. Protrusion of the blocks was varied row by row. The blocks within a same row had the same protrusion.

The graph of figure 6 shows the mean static pressure for water entries A, C, D and B. A is positioned at the top of the block, B at the bottom and C and D respectively on the upstream and downstream faces of the block. Protrusion was varied for each row. Protrusion is specified with three

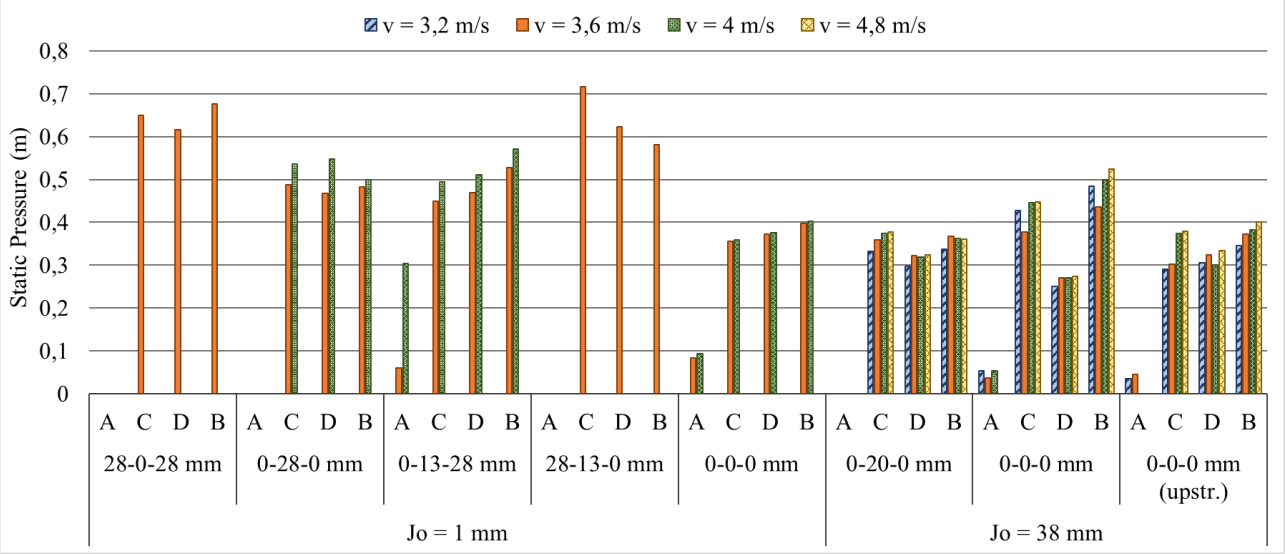

Figure 6: Static pressure on the instrumented block's faces

numbers: X-X-X. The first number indicates the protrusion in millimetres of the upstream row of blocks, the second number is the protrusion of the middle row and the last number is the protrusion of the downstream row of blocks. For example, 0-20-0 means the middle row has 20 mm protrusion from the channel surface and the upstream and downstream rows have no protrusion from the channel. The instrumented block was generally positioned in the middle row, except for the test where it is mentioned "upstr.". In this case, the instrumented block was positioned in the upstream row. Flow velocity used for each test is mentioned in the legend. Joint opening of 1 mm and of 38 mm are respectively the first and the second set of data (see horizontal axis).

For a joint opening of 1 mm, it is observed that a protrusion increases the static pressure on all faces, except on the top of the block, where a hydraulic jump is created when the middle row has a protrusion or when the upstream row has a protrusion. A difference is observed between an ascending staircase protrusion (0-13-28) and a descending staircase protrusion (28-13-0). For an ascending staircase protrusion, pressure under the block (B) is greater than pressure on the downstream face of the block (D) which is greater than the pressure on the upstream face of the block (C) (B>D>C). For a descending staircase, the opposite is observed (B<D<C).

For a joint opening of 38 mm, no significative difference of static pressure is observed between cases with or without protrusion. For all cases, mean static pressure is approximately equal to the mean static pressure for the case of a 1 mm joint opening without protrusion. In general, it is observed that pressure on the upstream face (C) and on the face under the block (B) are greater than pressure on the downstream face (D). Static pressure on top of the block (A) is always smaller. Indeed, water head above the block is the only pressure A records.

For all cases, velocity in the channel does not seem to have a great influence on the static pressure around the block. The only case when a slightly greater difference is observed is for the case with a 1 mm joint opening and a protrusion of 0-13-28 mm.

The graph of figure 7 shows the mean flow velocity recorded with a Pitot tube in the joints around the instrumented block. These tests were undergone only with a joint opening of 38 mm. Two cases were tested: with a 20 mm protrusion of the middle row (0-20-0) and without protrusion when the instrumented block was placed in the upstream row. The Pitot tube was always placed in the joint of the upstream face of the instrumented block.

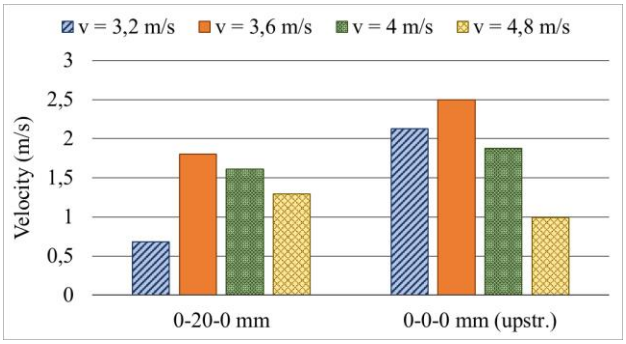

Figure 7: Mean flow velocity in the joints for a 38 mm joint opening

The graph of figure 7 shows that the mean flow velocity in the joints is greater for the case without protrusion that for the case with protrusion. It is also observed for the two configurations that mean flow velocity is at its maximum for a channel flow velocity of 3.6 m/s, and then decreases as the channel flow velocity increases. The minimum flow velocity in the joints corresponds to the minimum flow velocity of the channel.

The graph of figure 8 shows the variation of flow velocity over time in the joints for the case of a 38 mm joint opening, with a 20 mm protrusion of the middle row (0-20-0).

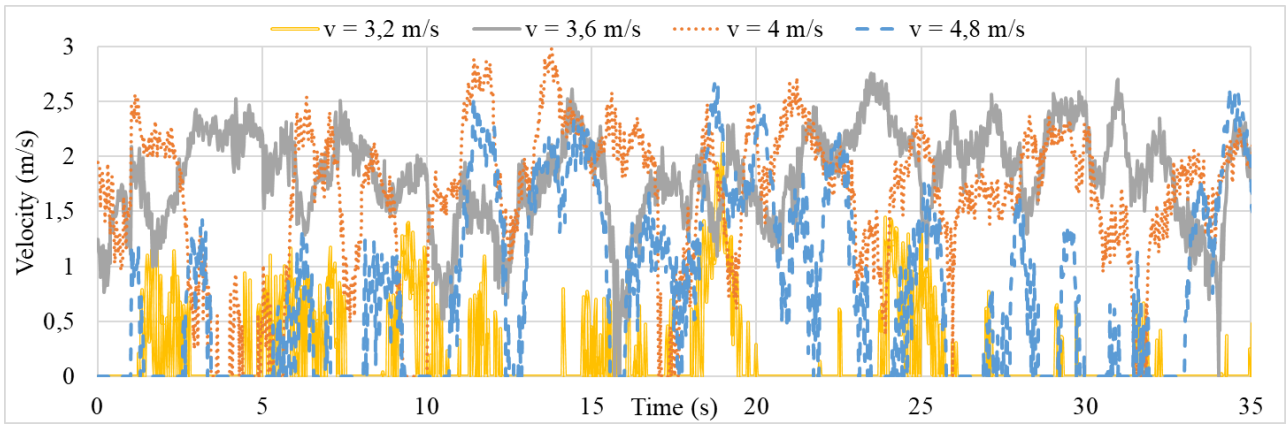

Figure 8: Variation of joint flow velocity over time for a 38 m joint opening and a 20 mm protrusion of the middle row (0-20-0)

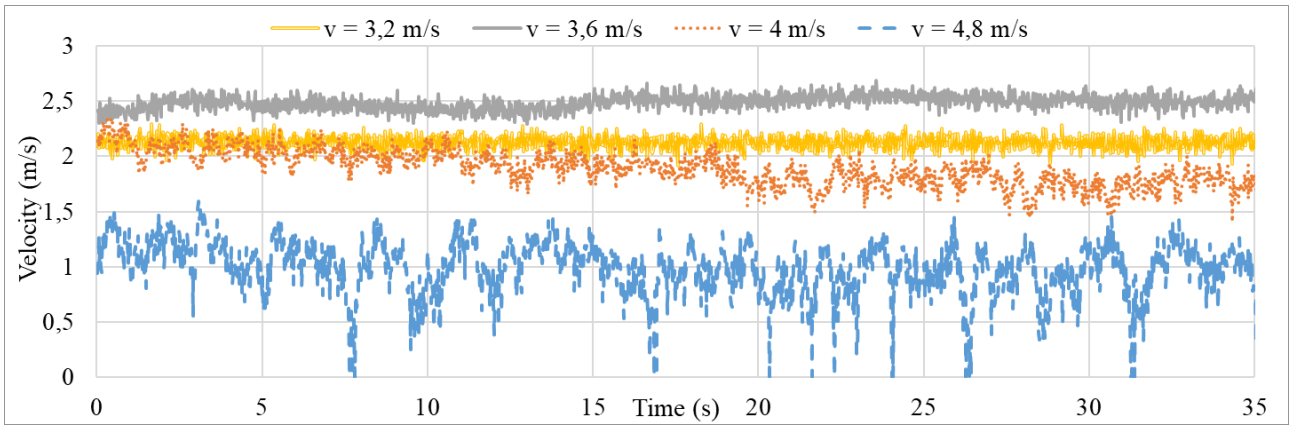

Figure 9: Variation of joint flow velocity over time for a 38 m joint opening, no protrusion and the instrumented block positioned on the upstream row.

The graph of figure 9 shows the variation of flow velocity over time in the joints for the case of a 38 mm joint opening, with no protrusion, when the instrumented block was positioned on the upstream row.

A noticeable difference of velocity variation is observed between figures 8 and 9. The flow velocity is much more varying for the case with protrusion that for the case without protrusion. The maximum flow velocity recorded is also greater for the case with protrusion than no protrusion. The case with protrusion shows that joint flow velocity fluctuations of 3.6 m/s, 4 m/s and 4.8 m/s channel velocities are very similar. Only joint flow velocity of 3.2 m/s channel flow velocity remains low. For the case without protrusion, joint velocity fluctuations are only observed for the 4.8 m/s channel flow velocity. This difference in flow velocity variation supports previous studies showing that rock mass erosion occurs when forces uplifting the block becomes greater than downward forces related to the block. This is shown to happen within a cycle of varying pressure (Bollaert and Schleiss 2002; Pan et al. 2014).

Lifting of blocks was observed for specific configurations, where the upstream row of blocks had a protrusion and when the blocks had a 1 mm joint opening. Uplifting occurred systematically when these conditions were fulfilled. The blocks were first toppled (the blocks' top going downstream and the blocks' bottom directed upstream). Then, pressure could build in the empty space created underneath the blocks. The nine blocks were then uplifted gradually in one mass. Increased flow velocity in the channel had for effect to increase the height of the blocks' uplift.

4 CONCLUSION AND FUTURE WORKS

A small-scale physical model was built according to a 1:40 Froude number scale of a real spillway channel. The purpose of this model is to study geometrical characteristics of the rock mass influencing its erodibility, as well as some geomechanical parameters of the rock mass and hydraulic characteristics of the flow in the spillway channel. Many years of future work are necessary to study the variety of possibilities that the small-scale physical model allows.

For now, the objective is to compare the effect of different joint opening and protrusion on static and dynamic pressure on the block's faces. Since the water entries measure only static water pressure, these water entries will be modified with elbows as outputs from the water entries on the block's faces and oriented against the direction of the flow. This should allow the pressure sensors to measure the total water pressure, and therefore to have a measure of flow velocity on each side of the block.

Results obtained so far indicates that the small-scale physical model is functional and that it is feasible to measure pressure on the block's faces with pressure sensors and flow velocity in the joints with a Pitot tube. The increased variation of the flow velocity in the joints for the case with a 38 mm joint opening and a 20 mm protrusion of the middle row (0-20-0 mm) compared to the case with the same joint opening but without protrusion tends to support previous studies on rock mass erodibility in flow channels.

5 ACKNOWLEDGMENTS

The authors would like to thank the research group R^{2}Eau for their helpful comments and suggestions, as well as the Natural Sciences and Engineering Research Council of Canada (NSERC) and Hydro-Québec, Uniper and Mitacs Inc. (#CRDPJ 537350 - 18, # IT22640) for funding the research.

6 REFERENCES

Annandale, G.W. 1995. Erodibility. Journal of Hydraulic Research, **33**(4): 471-494. doi:https://doi.org/10.1080/00221689509498656.

Annandale, G.W., Ruff, J.F., Wittler, R.J., and Lewis, T.M. Prototype Validation of Erodibility Index for Scour in Fractured Rock Media. *In* International Water Ressources Engineer Engineering Conference. Memphis, Tenessee 1998. American Society of Civil Engineers. pp. 1096-1101.

Bollaert, E., and Schleiss, A. 2002. Transient water pressures in joints and formation of rock scour due to high-velocity jet impact. Ph.D Thesis, EPFL-LCH.

Boumaiza, L., Saeidi, A., and Quirion, M. 2019. A method to determine relevant geomechanical parameters for evaluating the hydraulic erodibility of rock. Journal of Rock Mechanics and Geotechnical Engineering, **11**(5): 1004-1018. doi:https://dx.doi.org/doi:10.1016/j.jrmge.2019.04.002.

Boumaiza, L., Saeidi, A., and Quirion, M. 2021. A method to determine the relative importance of geological parameters that control the hydraulic erodibility of rock. Quarterly Journal of Engineering Geology and Hydrogeology, **54**(4): 2020-2154. doi:https://doi.org/10.1144/qjegh2020-154.

George, M., Sitar, N., and Sklar, L. Experimental evaluation of rock erosion in spillway channels. *In* 49th US Rock Mechanics / Geomechanics Symposium 2015. 2015. ARMA, San Francisco.

Kirsten, H. 1982. A classification system for excavation in natural materials. Civil Engineer in South Africa, **24**(7): 293-308.

Kirsten, H.A., Moore, J.S., Kirsten, L.H., and Temple, D.M. 2000. Erodibility criterion for auxiliary spillways of dams. International Journal of Sediment Research, **15**(1): 93-107. Available from https://pubag.nal.usda.gov/catalog/22534 [accessed 02-11-2020].

Koulibaly, A.S. 2021. Conception d'un modèle de laboratoire d'un évacuateur de crues pour étudier l'érosion des masses rocheuses. MSc Thesis, Université du Québec à Chicoutimi.

Pan, Y.-W., Li, K.-W., and Liao, J.-J. 2014. Mechanics and response of a surface rock block subjected to pressure fluctuations: A plucking model and its application. Engineering Geology, **171**: 1-10. doi:10.1016/j.enggeo.2013.12.008.

Pells, S. 2016. Erosion of Rocks in Spillways. Ph.D Thesis, Civil and Environmental Engineering, University of New South Wales.

Reinius, E. 1986. Rock erosion. International Water Power and Dam Construction, **38**(6): 43-48.

Van Schalkwyk, A., Jordaan, J., and Dooge, N. Erosion of rock in unlined spillways. *In* International Commission on Large Dams. Paris 1994. pp. 555-571.